

# Associative Morphological Memories for Spectral Unmixing

M. Graña, M.J. Gallego  
Dept. CCIA, UPV/EHU, San Sebastian, SPAIN  
(email:ccpgrrom@si.ehu.es)

**Abstract.** Unlimited storage and perfect recall of noiseless real valued patterns has been proved for Autoassociative Morphological Memories (AMM). However AMM's suffer from sensitivity to specific noise models, that can be characterized as erosive and dilative noise. On the other hand, Spectral Unmixing of Hyperspectral Images needs the prior definition of a set of Endmembers, which correspond to material spectra lying on vertices of a convex region covering the image data. These vertices can be characterized as morphologically independent patterns. We present a procedure that takes advantage of the AMM's noise sensitivity to perform Endmember spectra selection based on this characterization.

## 1 Introduction

Multispectral sensing allows the recognition of physical materials in image pixels, however as these image pixels are frequently a combination of materials, we need to decompose the pixel spectrum into their constituent material spectra. Hyperspectral sensor measurements in hundreds of spectral bands allow to perform such "spectral unmixing" [4]. The mixture of several spectra in a single pixel may be due to the spatial resolution of the sensor that implies that different land covers are included in the earth surface area whose radiance measurement are observed as an image pixel. This situation produces mixtures which, often, can be adequately modeled by a linear mixing model. In this paper we assume that the linear model is correct, and we introduce an approach that applies some properties of AMM's to the detection in hyperspectral images of pixel spectra that may serve as endmembers for spectral unmixing.

In short, Morphological Neural Networks are those that involve somehow the maximum and/or minimum (supremum and/or infimum) operators in their definition. The Associative Morphological Memories [6], [7], [8] are the morphological counterpart of the well known Hopfield Associative Memories [2].

---

The authors received partial support from projects of the Ministerio de Ciencia y Tecnologia TIC2000-0739-C04-02 and TIC2000-0376-P4-04

AMM's are constructed as correlation matrices computed by either Min or Max matrix product (denoted by symbols  $\boxtimes$  and  $\boxplus$  respectively). Dual constructions can be made using the dual Min and Max operators. The AMM's are very sensitive to specific types of noise (erosive and dilative noise). The notion of morphological independence and morphological strong independence was introduced in [8] to formalize the construction of AMM's robust against arbitrary noise following the kernel approach. Briefly, AMM's can robustly store and recall morphologically strongly independent sets of patterns. As endmembers for spectral unmixing are morphologically independent we propose a procedure that uses the AMM's to detect new endmembers from an hyperspectral image. The "learning" procedure is unsupervised and detects the endmembers in a single pass over the image.

The structure of the paper is as follows: In section 2 we review the definition of the linear mixing model. Lack of space prevents us from giving a review of AMM's. In section 3 we introduce our endmember selection algorithm for remote sensing hyperspectral images. In section 4 we discuss some experimental results of the proposed algorithm. In section 5 we summarize our conclusions and we propose future work directions.

## 2 The linear mixing model

The linear mixing model [4] can be expressed as follows:

$$\mathbf{x} = \sum_{i=1}^M a_i \mathbf{s}_i + \mathbf{w} = \mathbf{S}\mathbf{a} + \mathbf{w}, \quad (1)$$

where  $\mathbf{x}$  is the  $d$ -dimensional random vector that represents the pixel spectrum,  $\mathbf{S}$  is the  $d \times M$  matrix whose columns are the  $d$ -dimension endmembers  $\mathbf{s}_i, i = 1, \dots, M$ ,  $\mathbf{a}$  is the  $M$ -dimension fractional abundance vector, and  $\mathbf{w}$  is the  $d$ -dimensional additive sensor noise vector. The linear mixing model is subjected to two constraints on the abundance coefficients. First, to be physically meaningful, all abundance coefficients must be non-negative  $a_i \geq 0, i = 1, \dots, M$ . Second, to account for the entire composition, the abundance coefficients must be fully additive  $\sum_{i=1}^M a_i = 1$ .

The task of endmember determination is the focus of this paper. In an already classical paper [1], Craig starts with the observation that the scatter plots of remotely sensed data are tear shaped or pyramidal, if two or three spectral bands are considered. The apex lies in the so-called dark point. The endmember detection becomes the search for non-orthogonal planes that enclose the data forming a minimum volume simplex, hence the name of the method. The method is computationally expensive and requires the prior specification of the number of endmembers. Another step to the automatic endmember detection is the Conical Analysis method proposed in [3] and applied to target detection. The extreme points in the data after a Principal Component transform are the searched for endmember spectra. Another approach is the modelling by

Markov Random Fields and the detection of spatially consistent regions whose spectra will be assumed as endmembers [5].

Once the endmembers have been determined the unmixing is the computation of the matrix inversion that gives the fractional abundance of each endmember in each pixel spectra and, therefore, the spectral unmixing. The simplest approach is the unconstrained least squared error estimation given by:

$$\hat{\mathbf{a}} = (\mathbf{S}^T \mathbf{S})^{-1} \mathbf{S}^T \mathbf{x}. \quad (2)$$

The abundance coefficients that result from this computation do not necessarily fulfill the non-negativity and full additivity constraints. It is possible to enforce each constraint separately, but it is rather difficult to enforce both simultaneously [4]. As our aim is to test an endmember spectra selection procedure, we will use unconstrained estimation (2) to compute the abundance images. We will scale and shift the intensity of the abundance images to present our results.

### 3 The detection of spectral endmembers

Under a geometrical interpretation, the endmembers of a given hyperspectral image assuming the linear mixture model correspond to the vertices of the minimal simplex that encloses the data points. On the other hand, the region of the space defined by a set of vectors which are morphologically independent in both the erosive and dilative senses simultaneously, is a high dimensional box that we want to approximate the minimal simplex enclosing the data points. Let us denote  $\{\mathbf{f}(i, j) \in \mathbb{R}^d; i = 1, \dots, n; j = 1, \dots, m\}$  the  $d$ -bands hyperspectral image,  $\boldsymbol{\mu}$  and  $\boldsymbol{\sigma}$  the vectors of the mean and standard deviations of each band computed over the image,  $\alpha$  the noise correction factor and  $E$  the set of endmembers discovered. The noise amplitude in (1) is estimated as  $\boldsymbol{\sigma}$ , the patterns are corrected by the addition and subtraction of  $\alpha\boldsymbol{\sigma}$ , before being presented to the AMM's. The confidence level  $\alpha$  controls the amount of flexibility in the discovering of new endmembers. Let us denote by the expression  $\mathbf{x} > \mathbf{0}$  the construction of the binary vector ( $\{b_i = 1 \text{ if } x_i > 0; b_i = 0 \text{ if } x_i \leq 0\}; i = 1, \dots, n$ ).

The steps in the procedure are the following:

1. Compute the zero mean image  $\{\mathbf{f}^c(i, j) = \mathbf{f}(i, j) - \boldsymbol{\mu}; i = 1, \dots, n; j = 1, \dots, m\}$ .
2. Initialize the set of endmembers  $E = \{\mathbf{e}_1\}$  with a pixel spectrum randomly picked from the image. Initialize the set of morphologically independent binary signatures  $X = \{\mathbf{x}_1\} = \{(e_k^1 > 0; k = 1, \dots, d)\}$
3. Construct the erosive ( $M_{XX}$ ) and dilative ( $W_{XX}$ ) AMM's based on the morphologically independent binary signatures in  $X$ .
4. For each pixel  $\mathbf{f}^c(i, j)$ 
  - (a) compute the vector of the signs of the Gaussian noise corrections  $\mathbf{f}^+(i, j) = (\mathbf{f}^c(i, j) + \alpha\boldsymbol{\sigma} > \mathbf{0})$  and  $\mathbf{f}^-(i, j) = (\mathbf{f}^c(i, j) - \alpha\boldsymbol{\sigma} > \mathbf{0})$

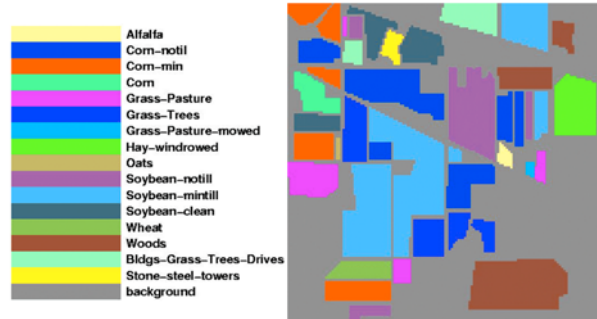


Figure 1: Ground truth of the Indian Pines image.

- (b) compute  $y^+ = M_{XX} \boxtimes \mathbf{f}^+(i, j)$
  - (c) compute  $y^- = W_{XX} \boxtimes \mathbf{f}^-(i, j)$
  - (d) if  $y^+ \notin X$  and  $y^- \notin X$  then  $\mathbf{f}^c(i, j)$  is a new endmember to be added to  $E$ , go to step 3 and resume the exploration of the image.
  - (e) if  $y^+ \in X$  and  $\mathbf{f}^c(i, j) > \mathbf{e}_{y^+}$  the pixel spectral signature is more extreme than the stored endmember, then substitute  $\mathbf{e}_{y^+}$  with  $\mathbf{f}^c(i, j)$ .
  - (f) if  $y^- \in X$  and  $\mathbf{f}^c(i, j) < \mathbf{e}_{y^-}$  the pixel is more extreme than the stored endmember, then substitute  $\mathbf{e}_{y^-}$  with  $\mathbf{f}^c(i, j)$ .
5. The final set of endmembers is the set of original spectral signatures  $\mathbf{f}(i, j)$  of the pixels selected as members of  $E$ .

## 4 Experimental results

The spectra used for this work correspond to the Indian Pines 1992 image obtained by the Airborne Visible/Infrared Imaging Spectrometer (AVIRIS) developed by NASA JPL which has 224 contiguous spectral channels covering a spectral region from 0.4 to 2.5  $\mu\text{m}$  in 10 nm steps. It is a 145 by 145 pixel image with 220 spectral bands that contains a distribution of two-thirds of agricultural land and one-third of forest and other elements (two highways, a railroad track, some houses and smaller roads). The available image ground truth designates 16 mutually exclusive classes of land cover. Figure 1 shows the ground truth as given in [9]. Comparison of the results of careful supervised classification [9] with the abundance images in figure 2 resulting from the detected endmembers, confirm the validity of the abundance images and explain their discrepancies relative to the ground truth areas.

We have applied our method for endmember detection on the result of performing a Principal Component Analysis (PCA) pixel spectra dimension reduction from 220 to 11 coefficients. Working with the PCA reduced data has

the advantage of reducing the computation requirements, however it is not clear whether significant information is lost in the dimension reduction process. An important remark: the endmember spectra are taken from the original image, not from the PCA reconstruction. The PCA coefficients image is used for the selection of the pixels whose spectra will be selected. We have obtained 8 endmembers. The number of endmembers found depends on the initially chosen endmember and on the control parameter  $\alpha$ , which was empirically set to 0.2 in this experiment. The spectral unmixing based on the endmember spectra found does not produce results with any physical meaning, but their examination is our qualitative validation of the endmember identification process, and it is useful because there is no clear quantitative alternative to validate the approach. These abundance images show that the procedure really discovers meaningful spectra, and that they are consistent even after PCA transformations of the data. The abundance images are presented in figure 2. Consider, for example, the steel towers identified in the ground truth. It is not difficult to find in the abundance image collections, ones that highlight specially this structure. There are even "negative" recognition results in the form of negative (black) abundance pixels. The endmember spectrum corresponding to the abundance image 5 in figure 2 may be considered as good steel detector. Curiously enough, the roads are also clearly drawn in this abundance image. Our interpretation is that this spectrum identified as the endmember 5 corresponds to a generic opposite to the vegetal cover spectra. The abundance image 3 of fig. 2, shows good detection of cultivated land and negative abundance response in woods areas. If we consider the fact that due to the early growth stages most of the surface area corresponding to a pixel in the cultivated land is bare soil, we may assume that the endmember that generates this abundance image corresponds to soil cover spectra. On the other hand, abundance image 7 in both figures detects clearly woods and tree canopy areas. The detection in these images agrees with the ground truth in 1. The background class is identified also with woods in some areas of these abundance images. This result agrees with the results of careful supervised classification experiments reported in [9].

## 5 Conclusions and Further Work

We have proposed an algorithm for endmember detection in hyperspectral images taking advantage of the noise sensitivity of the Autoassociative Morphological Memories (AMM). The procedure does not need the a priori setting of the number of endmembers. Its flexibility in the discovering of endmembers is controlled by the amount of noise correction introduced in the pixel spectral signature. Experimental results on the Indian Pines image have demonstrated that the procedure gives a reasonable number of endmembers with little tuning of the control parameter ( $\alpha$ ), and that these endmembers have physical meaning and that they may serve for the analysis of the image.

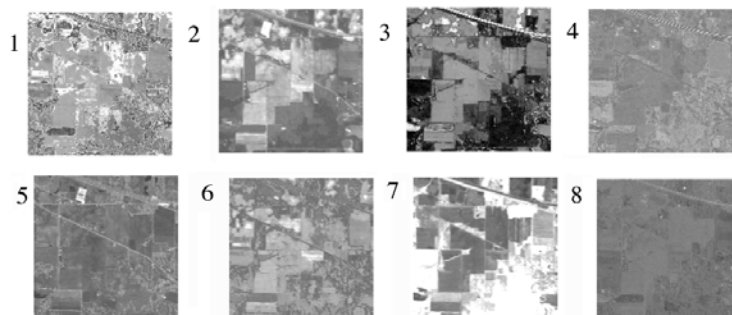


Figure 2: Abundance images obtained by the proposed procedure on the PCA coefficients of the pixels.

## References

- [1] Craig M., (1994) Minimum volume transformations for remotely sensed data, *IEEE Trans. Geos. Rem. Sensing*, 32(3):542-552
- [2] Hopfield J.J., (1982) Neural networks and physical systems with emergent collective computational abilities, *Proc. Nat. Acad. Sciences*, vol. 79, pp.2554-2558,
- [3] Ifarraguerri A., C.-I Chang, (1999) Multispectral and Hyperspectral Image Analysis with Convex Cones, *IEEE Trans. Geos. Rem. Sensing*, 37(2):756-770
- [4] Keshava N., J.F. Mustard Spectral unmixing, *IEEE Signal Proc. Mag.* 19(1) pp:44-57 (2002)
- [5] Rand R.S., D.M. Keenan (2001) A Spectral Mixture Process Conditioned by Gibbs-Based Partitioning, *IEEE Trans. Geos. Rem. Sensing*, 39(7):1421-1434
- [6] Ritter G. X., J. L. Diaz-de-Leon, P. Sussner. (1999) Morphological bidirectional associative memories. *Neural Networks*, Volume 12, pages 851-867,
- [7] Ritter G. X., P. Sussner, J. L. Diaz-de-Leon. (1998) Morphological associative memories. *IEEE Trans. on Neural Networks*, 9(2):281-292,
- [8] Ritter G.X., G. Urcid, L. Iancu, (2002) Reconstruction of patterns from moisy inputs using morphological associative memories, *J. Math. Imag. Vision* submitted
- [9] Tadjudin, S. and D. Landgrebe, (1999) Covariance Estimation with Limited Training Samples, *IEEE Trans. Geos. Rem. Sensing*, 37(4):2113-2118,